Available online at www.sciencedirect.com
ScienceDirect
Journal of Nuclear Materials 367–370 (2007) 147–152
journal of nuclear materials
www.elsevier.com/locate/jnucmat

Microstructural analysis on JLF-1 steel tested by fatigue deformation

Huailin Li [a,c], Arata Nishimura [b], Takeo Muroga [b], Takuya Nagasaka [b,*]

[a] The Graduate University for Advanced Studies, Toki, Gifu 509-5292, Japan
[b] Fusion Engineering Research Center, National Institute for Fusion Science, Oroshi, Toki, Gifu 509-5292, Japan
[c] China Institute of Atomic Energy, Beijing 012413, China

Abstract

Microstructural changed of JLF-1 steel induced by static tensile loading and tension/compression cyclic loading was investigated following tensile and low cycle fatigue tests in vacuum at elevated temperature. Secondary cracks in radial direction were observed on the fracture surface of the tensile specimen at RT. Initial cyclic hardening followed by cyclic softening was observed during fatigue at RT and 673 K. In contrast, only cyclic softening was observed at 873 K. Transmission electron microscopy images of specimens with a total strain range $\Delta\varepsilon_t = 1.8\%$ at RT, 673 K and 873 K showed that cyclic softening is caused by the reduction of the dislocation density and increment of lath width resulted by partial annihilation of original lath boundaries and cyclic deformation. The peak stress and lath width imply qualitative relationships that correlate with the number of cycles.

1. Introduction

A reduced-activation ferritic/martensitic steel, JLF-1, is one of the candidate alloys for blanket structure components of fusion reactors [1]. For the application as a structural material, it is necessary to evaluate tensile and low cycle fatigue (LCF) properties at high temperature [2].

Mechanical properties of martensitic steels are strongly related to their complex microstructure [3]. Since the tensile and fatigue properties are key design issues for structural components of fusion reactor, it is essential to understand the microstructural changes under static or cyclic deformation.

In this study, the microstructural changes of JLF-1 steel induced by static tensile loading and strain controlled tension/compression cyclic loading were investigated following the tensile and low cycle fatigue tests using engineering sized cylindrical specimens in vacuum at elevated temperature. The fractography of tensile specimens was observed in a scanning electron microscopy (SEM). The 3 mm diameter thin foils for transmission electron microscopy (TEM) were prepared from the as-received material and the center of the LCF specimens.

* Corresponding author. Tel.: +81 572 58 2252; fax: +81 572 58 2676.
E-mail address: Nagasaka@ms.nifs.ac.jp (T. Nagasaka).

0022-3115/$ - see front matter © 2007 Published by Elsevier B.V.
doi:10.1016/j.jnucmat.2007.03.152

2. Experimental procedure

2.1. Materials

The chemical composition of the JLF-1 steel plate in wt% is Fe–0.10C–0.05Si–0.45Mn–0.003P–0.002S–0.003Al–8.85Cr–01.99W–0.20V–0.080Ta–0.0231N–0.0002B–<0.01Ni–<0.05Cu–<0.001Mo–<0.002Nb. The plate was 15 mm thick and heat-treated as follows: 1323 K/3.6 ks/air cooled (normalizing) and 1052 K/3.6 ks/air cooled (tempering) [4]. The microstructure is tempered martensite [5].

2.2. Tensile test

The tensile tests were carried out from RT to 873 K at a strain rate of 0.1%/s and 0.02%/s in vacuum ($\leqslant 5\times10^{-3}$ Pa) using engineering size cylindrical specimens with a 12.5 mm gauge length within the 8 mm in diameter, and 30 mm in length reduced section of the specimen. Two thermocouples (0.32 mm in diameter) were welded in the gage length on the specimen. The temperature difference of the two thermocouples was kept less than 3 K.

2.3. Fatigue test

The engineering size cylindrical specimens also had a 12.5 mm gauge length within an 8 mm in diameter and 20 mm in length reduced section. These were used to carry out the LCF test at RT, 673 K and 873 K [6,7]. A fully reversed strain controlled triangular push–pull wave was applied with strain rate of 0.1%/s.

To investigate the microstructure change during fatigue at elevated temperature, tests were terminated for some specimens at the 10th and 500th cycle with a total strain range $\Delta\varepsilon_t = 1.8\%$ at 673 K and 873 K.

2.4. Microstructural observation

The fractography of tensile specimens was observed with scanning electron microscopy. The 3 mm diameter thin foils for TEM were prepared from the as-received material and the center of the LCF specimens of total strain range $\Delta\varepsilon_t = 1.8\%$ at RT, 673 K and 873 K. All thin foils were polished to less than 0.1 mm in thickness with #1500 emery paper, followed by electropolishing to perforation for TEM examination.

3. Results

3.1. Tensile tests

The change in yield stress (YS), ultimate tensile stress (UTS) and the reduction of area (RA) are shown as a function of temperature in Figs. 1 and 2. The strain rate does not affect YS, UTS and RA significantly. RA increased and the strain hardening decreased significantly between 673 K and 873 K. The UTS of JLF-1 drops to about 300 MPa at 873 K.

Fig. 3 shows the SEM images of fracture surfaces of the tensile specimens at strain rates of 0.1%/s at RT, 0.1% and 0.02%/s at 673 K and 873 K. Secondary cracks in the radial direction were observed on

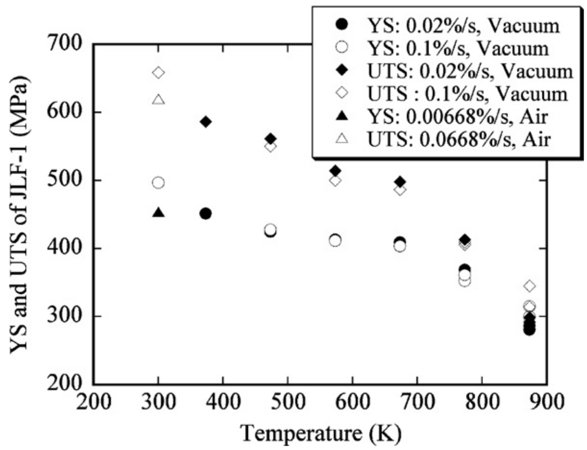

Fig. 1. Temperature dependence of YS and UTS. (The data in air are from [5].)

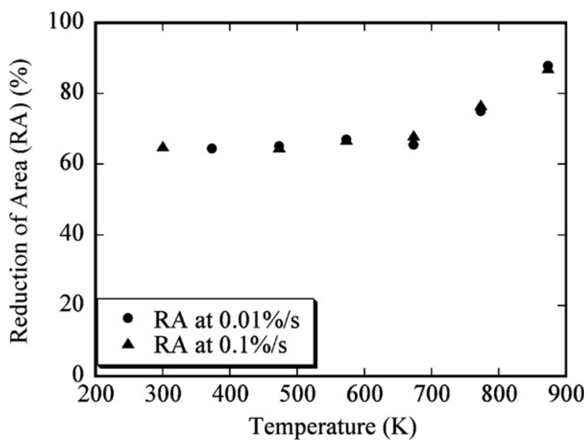

Fig. 2. Temperature dependence of RA change.

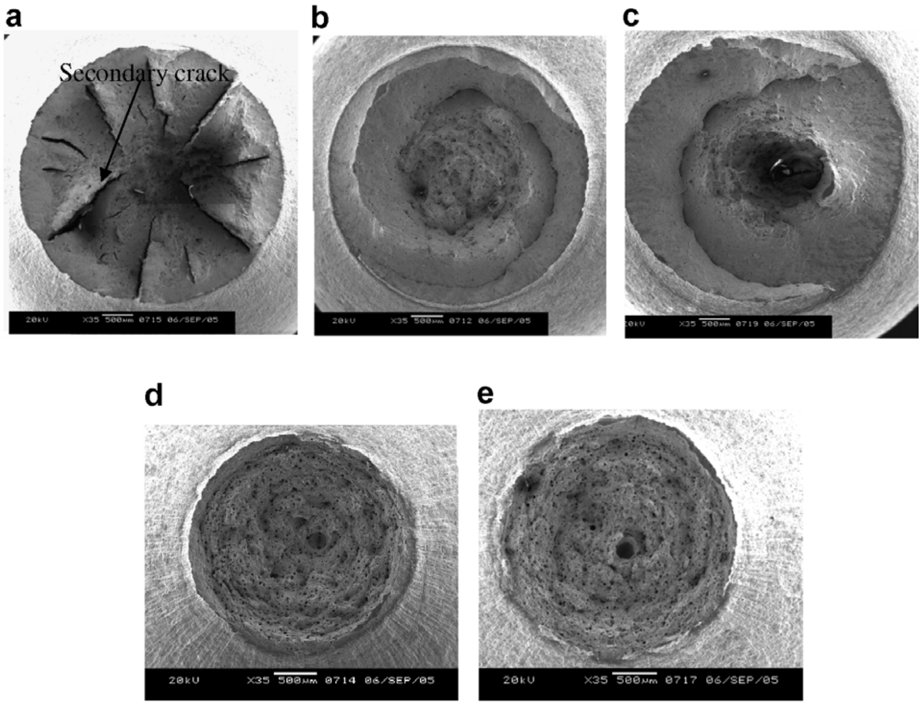

Fig. 3. SEM images of the fracture surfaces of the tensile specimens: (a) RT, 0.1%/s; (b) 673 K, 0.1%/s; (c) 673 K, 0.02%/s; (d) 873 K, 0.1%/s and (e) 873 K, 0.02%/s.

the fracture surface at RT, which were formed by tangential stresses during necking where a tri-axial stress applies [5]. Cup and cone fracture was observed in the specimens tested at high temperature. A high density of dimples was observed at 873 K, implying enhanced ductility at high temperature.

3.2. Fatigue tests

The change in peak tensile stress during fatigue tests at RT, 673 K and 873 K at a total strain range $\Delta\varepsilon_t = 1.8\%$ is shown in Fig. 4. The peak stresses at RT and 673 K increased initially and then decreased gradually until the final failure occurred, which demonstrates the initial cyclic hardening which is followed by cyclic softening. This phenomenon was also reported in the case of JLF-1 at RT in air, which was considered to be due to dislocation pile up with tangling [4]. At 873 K, only cyclic softening was observed.

3.3. TEM images

TEM images of the as-received material and the specimens after fatigue tests at a total strain range

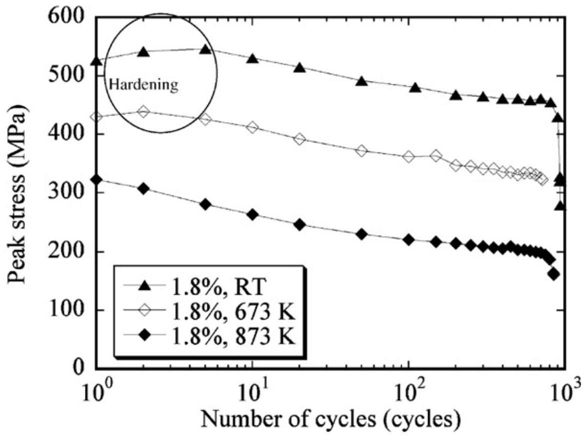

Fig. 4. Change in peak stress during fatigue.

$\Delta\varepsilon_t = 1.8\%$ at RT were shown in Fig. 5. The as-received material consists of a martensitic structure, with the carbide distribution along the lath boundary. After fatigue at RT, the lath width became wider. Assuming that carbides inside the subgrains indicate the position of the original lath boundary [8], the microstructures suggest that partial annihilation of original lath boundaries occurred during cyclic deformation. Further investigation showed

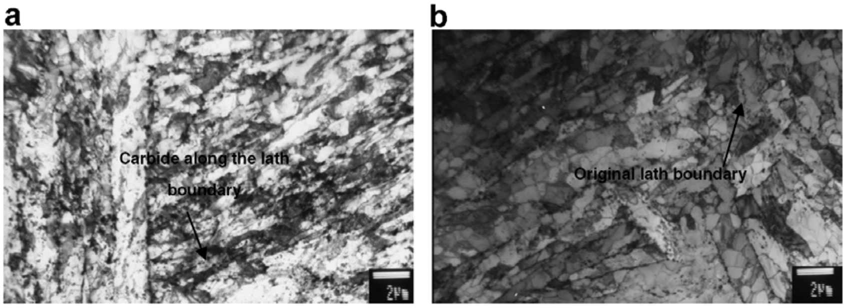

Fig. 5. Effects of cyclic deformation on microstructure at RT. (a) Base metal and (b) 936th cycle at RT, 1.8%.

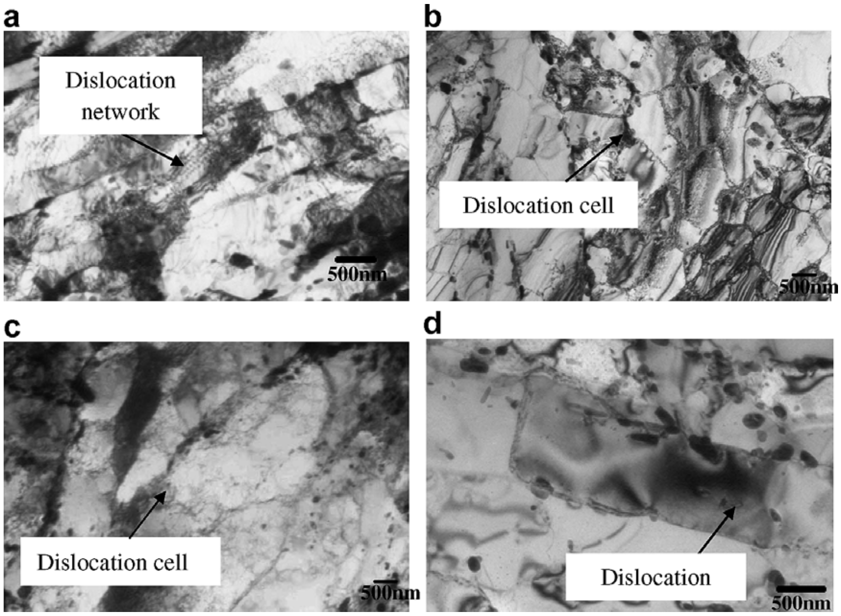

Fig. 6. Cyclic deformation and temperature effect on dislocation structure. (a) Base metal; (b) 936th cycle at RT, 1.8%; (c) 10th cycle at 673 K, 1.8% and (d) 716th cycle at 673 K, 1.8%.

that partial annihilation of original lath boundaries and resulting increase in lath width were enhanced with temperature, as will be shown later.

The TEM images of dislocations before and after fatigue are shown in Fig. 6. The dislocation structure was changed from network in the as-received material to cell after cyclic deformation at RT. The dislocation density was also reduced with the cyclic deformation. At 673 K, a loose cell structure was observed at 10th cycle. However the cell structure did not remain following fatigue and only few dislocations were observed at the TEM images at the 500th cycle and the final failure at 673 K. At 873 K, the cell structure was not observed; the dislocation density decreased with cycles.

4. Discussion

4.1. Cyclic softening

Similar to F82H [9] and Eurofer 97 [10], JLF-1 showed cyclic softening at RT, 673 K (after initial cyclic hardening) and 873 K during LCF test in vacuum. The cyclic softening is caused by the yield stress decrease during fatigue [7]. The yield stress (σ_y) of martensitic steel can be separated into several components [11].

$$\sigma_y = \sigma_D + \sigma_b + \cdots \quad (1)$$

The relationship between dislocation strengthening (σ_D) and dislocation density (ρ) is

$$\sigma_D \propto \rho^{0.5}. \quad (2)$$

The relationship between polycrystal effect (σ_b) and lath width (d) is

$$\sigma_b \propto d^{-1}. \quad (3)$$

TEM images showed the reduction of dislocation density, increase of lath width and partial annihilation of original lath boundaries during fatigue test. Assuming partial annihilation of original lath boundaries is responsible for causing the increased lath width, the reduction of dislocation density and increasing of lath width resulted from partial annihilation of original lath boundaries and cyclic deformation will cause the yield stress to decrease. Thus, the cyclic softening was observed during fatigue.

4.2. Carbide coarsening

It was reported that the carbide ($M_{23}C_6$) coarsening was the one of the factors for the acceleration of the cyclic softening during fatigue of AISI H11 above 873 K [3]. However, such a phenomenon was not observed in this study. The average size of $M_{23}C_6$ carbides were in the range of 95–105 nm, did not change significantly even after fatigue at high temperature.

4.3. Lath width-better correlation parameter for cyclic softening

The peak stress is an important parameter for detecting cyclic softening during a LCF test. Several microstructural parameters may be correlated with this phenomenon: (1) Dislocation cell structure – it was reported that the cyclic stress depends on the dislocation cell size [3,12,13]. But in present study, the cell structure is not stable at 673 K, and not observed at 873 K. This means there are limits to the temperature range where this parameter may be applicable. (2) Dislocation density – the dislocation density is decreased during fatigue testing from RT to 873 K. But it is not easy to quantity the change in density because the microstructure of the tempered martensitic phase is not homogeneous. (3) Carbide size – some researchers pointed out carbide ($M_{23}C_6$) coarsening was observed during fatigue [3]. But in present study, the size of $M_{23}C_6$ carbides did not change significantly. (4) Lath width – according to [14], the lath width was measured from the TEM images as an average separation of the lath boundary. The change in cyclic stress with lath width was shown in Fig. 7. The data showed a tendency for the stress to decrease and lath width to increase during a fatigue test. Based on the above analysis and Figs. 4 and 7, the peak stress and lath width appeared to correlate with the number of cycles at 673 K and 873 K. However, further characterization of microstructure is needed to establish the relationship.

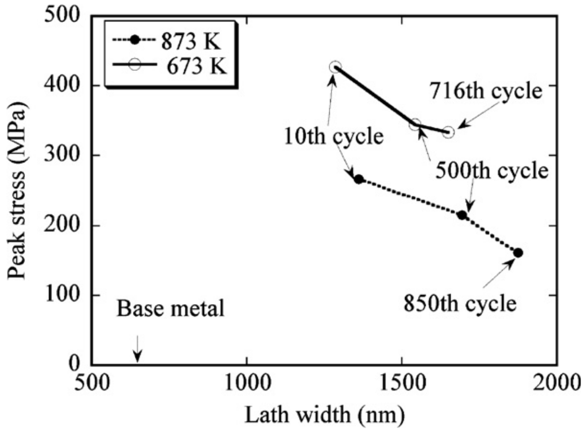

Fig. 7. Peak stress as a function of lath width at a total strain range $\Delta\varepsilon_t = 1.8\%$ at 673 K and 873 K.

5. Summary

(1) Tensile tests were carried out form RT to 873 K at strain rates of 0.1%/s and 0.02%/s in vacuum. The strain rate did not affect YS, UTS and RA as far as the tests performed in this study. Secondary cracks in the radial direction were observed on the fracture surface at RT, which were formed by tangential stress during necking where the tri-axial stress applies.

(2) Initial cyclic hardening followed by cyclic softening was observed at RT and 673 K. At 873 K, only cyclic softening was observed. TEM images at total strain range $\Delta\varepsilon_t = 1.8\%$ at RT, 673 K and 873 K showed that the cyclic softening is caused by reduction of the dislocation density and increase of lath width resulting from partial annihilation of original lath boundaries due to cyclic deformation. The size of $M_{23}C_6$ carbides in JLF-1 did not change significantly during LCF test even at high temperature.

(3) Compared with dislocation structure and carbide size, it seems that the lath width is a

better parameter to indicate cyclic softening. The peak stress and lath width at a total strain range $\Delta\varepsilon_t = 1.8\%$ at 673 K and 873 K may be correlated with the number of cycles.

Acknowledgements

The work was supported by NIFS Budget Code NIFS05UCFF005. The authors are thankful to Professor H. Watanabe of RAM, Kyushu University, for TEM observation.

References

[1] A. Kohyama, Y. Kohno, K. Asakura, et al., J. Nucl. Mater. 212–215 (1994) 684.
[2] K. Shiba, A. Hishinuma, A. Kohyama, et al., JAERI-Tech 97-08.
[3] N. Mebarki, D. Delagnes, P. Lamesle, et al., Mater. Sci. Eng. A 387–389 (2004) 171.
[4] A. Nishimura, T. Nagasaka, N. Inoue, et al., J. Nucl. Mater. 283–287 (2000) 677.
[5] A. Nishimura, N. Inoue, T. Muroga, J. Nucl. Mater. 258–263 (1998) 1242.
[6] H. Li, A. Nishimura, T. Nagasaka, et al., in: JCS-8, October 4–8, 2004, Sendai, Japan. p. 35.
[7] H. Li, A. Nishimura, T. Nagasaka, et al., Fus. Eng. Des. 81 (2006) 241.
[8] A.F. Armas, C. Petersen, R. Schmitt, et al., J. Nucl. Mater. 329–333 (2004) 252.
[9] T. Ishii, K. Fukaya, Y. Nishiyama, et al., J. Nucl. Mater. 258–263 (1998) 1183.
[10] A.F. Armas, C. Petersen, R. Schmitt, et al., J. Nucl. Mater. 307–311 (2002) 509.
[11] Q. Li, Mater. Sci. Eng. A 361 (2003) 385.
[12] H.J. Chang, J.J. Kai, J. Nucl. Mater. 191–194 (1992) 836.
[13] Y. Ei-Madhoun, A. Mohamed, M.N. Bassim, Mater. Sci. Eng. A 359 (2004) 220.
[14] N. Inoue, T. Muroga, A. Nishimura, et al., J. Nucl. Mater. 258–263 (1998) 1248.